World Academy of Science, Engineering and Technology
International Journal of Materials and Metallurgical Engineering
Vol:14, No:8, 2020

Comparative Parametric Analysis on the Dynamic Response of Fibre Composite Beams with Debonding

Indunil Jayatilake, Warna Karunasena

***Abstract*—**Fiber Reinforced Polymer (FRP) composites enjoy an array of applications ranging from aerospace, marine and military to automobile, recreational and civil industry due to their outstanding properties. A structural glass fiber reinforced polymer (GFRP) composite sandwich panel made from E-glass fiber skin and a modified phenolic core has been manufactured in Australia for civil engineering applications. One of the major mechanisms of damage in FRP composites is skin-core debonding. The presence of debonding is of great concern not only because it severely affects the strength but also it modifies the dynamic characteristics of the structure, including natural frequency and vibration modes. This paper deals with the investigation of the dynamic characteristics of a GFRP beam with single and multiple debonding by finite element based numerical simulations and analyses using the STRAND7 finite element (FE) software package. Three-dimensional computer models have been developed and numerical simulations were done to assess the dynamic behavior. The FE model developed has been validated with published experimental, analytical and numerical results for fully bonded as well as debonded beams. A comparative analysis is carried out based on a comprehensive parametric investigation. It is observed that the reduction in natural frequency is more affected by single debonding than the equally sized multiple debonding regions located symmetrically to the single debonding position. Thus it is revealed that a large single debonding area leads to more damage in terms of natural frequency reduction than isolated small debonding zones of equivalent area, appearing in the GFRP beam. Furthermore, the extents of natural frequency shifts seem mode-dependent and do not seem to have a monotonous trend of increasing with the mode numbers.

***Keywords*—**Debonding, dynamic response, finite element modelling**,** FRP beams.

I. Introduction

FRP composite materials have been increasingly considered for structural applications by the civil engineering construction industry due to their outstanding properties including high specific strength and stiffness, resistance to corrosion, resistance to fire, high durability and reduction in the carbon footprint in the construction industry. The use of thin and stiff face sheets and a thick but lightweight core of composite sandwiches offers the designer of the structure with the capacity to control the flexural rigidities and yet to keep the global weight of the structure way below the weight of its monolithic alternatives [1]. Hence, FRP composites make up a class of advanced structural materials possessing a huge potential for their use in civil engineering, both for the rehabilitation of existing structures and for constructing new structures [2].

While the relatively high production and material costs are considered as major drawbacks preventing FRP composites to be fully embraced for structural applications, when the cost of the structures is considered over its whole life cycle, the enhanced durability qualities of FRP material can make them the most cost-effective material in many instances [3].

One of the main concerns in sandwich composites is that their load carrying capacity may be significantly reduced by local damage (debonding) between the face sheet and the core [4]. The causes of debonding usually include flaws in the manufacturing procedure, the capability for water absorption of cellular types of the core followed by recurrent cycles of freezing and thawing at the interface between face sheet and core and low-velocity impacts and stress concentrations due to localized loading [5]. According to [5], since debonding is an inherent potential cause for structural failure in sandwich panels, detailed knowledge about its influence on the dynamic behaviour of the sandwich composite is highly required. Even though the dynamic behaviour of undamaged composite sandwiches is the subject of extensive research, papers reported on the dynamic behaviour of debonded composite sandwich beams are limited. A comprehensive review of the recent research and developments in the dynamic analysis of sandwich panels with face sheet-to-core debonding is presented in [5].

A structural GFRP composite sandwich panel made from E-glass fibre skin and a modified phenolic core has been manufactured in Australia for civil engineering applications such as floors, pedestrian bridges and railway sleepers. Fig. 1 shows the preparation of these glue-laminated novel sandwich beams.

(a) Gluing sandwich panels (b) Cutting of sandwich beams

Fig. 1 Preparation of glue-laminated composite sandwich beams [6]

Several authors have investigated free vibration behaviour

I. Jayatilake is with the Civil Engineering Division, TAFE Queensland, Brisbane Region and School of Civil Engineering and Surveying, University of Southern Queensland, Toowoomba, QLD 4350, Australia (phone: +61420299980; e-mail: Indunil.Jayatilake@tafe.qld.edu.au)

W. Karunasena is with the School of Civil Engineering and Surveying, University of Southern Queensland, Toowoomba, QLD 4350, Australia (e-mail: Karu.Karunasena@usq.edu.au).

for the full bonded GFRP panels. Manalo et al. [7] did a comprehensive experimental study of the flexural behaviour of this GFRP sandwich test beams with a nominal thickness of 20 mm in flatwise and the edgewise positions. The fibre composite skin of this GFRP sandwich is made up of two plies of stitched bi-axial (0/90) E-CR glass fibre fabrics, and the modified phenolic foam core is a proprietary formulation by LOC Composites Pty. Ltd., Australia [7]. Islam and Aravinthan [8] examined the behaviour of this GFRP sandwich floor panel as two-span continuous floor panel and found that the panel shows a similar behaviour under point load and distributed load and also that there is no major effect of the type of fixity on the overall behaviour. Awad et al. [9] carried out an investigation of the free vibration behaviour of the fully bonded innovative GFRP sandwich panels using experimental and numerical approaches. The investigation was done on the GFRP sandwich floor panels by varying panel span, fibre orientation and restraint type. It was found that simply restraint panels had the lowest natural frequency while glue restraint panel had the highest frequency. Although the design engineers have accepted the GFRP sandwich panel to be used as a structural member due to its good mechanical properties, there is a lack of information about the free vibration behaviour of the GFRP sandwich floor panel [9]. A study on the free vibration behaviour of debonded sandwich plates using a 2D model was done by Karunasena [10]. The author examined the deviations in natural frequency due to various amounts of debonding along the glue line in a four layer laminated fibre composite sandwich plate structure using 2D FE modelling. In the Australian context, although experimental and numerical research has been conducted on the examination of the free vibration behaviour of the fully bonded GFRP sandwich panels, papers reported on the dynamic behaviour of debonded composite sandwiches are very limited.

II. Materials and Properties

The 300 mm long GFRP test beam used by Manalo et al. [7] for his experimental study (comprising of 2 mm top and bottom skins and a 16 mm middle core) has been selected for the initial investigation. Small test beams have been first used and modelled for the verification and initial modelling, and these test specimen sizes are then extended to a practical beam size (3 m long beam) for full scale modelling. The results of the model verification including analysis for small test beams are reported in [11]. Present paper deals with a comprehensive comparative parametric dynamic analysis for the 3 m long GFRP beam with single and multi-debonding. Mechanical properties of the GFRP beam used for the present analysis are given in Table I.

In this analysis, a composite sandwich beam with core bounded by top and bottom skins with a finite debonding between the top skin and the core is considered. The geometric dimensions of the beam and the debonding length and location are as defined in Fig. 2.

TABLE I
Mechanical Properties of the GFRP Beam Skin and Core [11]

Property	Skin	Core
Young's modulus along long direction (MPa)	12360	1350
Young's modulus in transverse direction (MPa)	10920	1350
Poisson's ratio	0.3	0.2
Density (kg/m^3)	1425	950

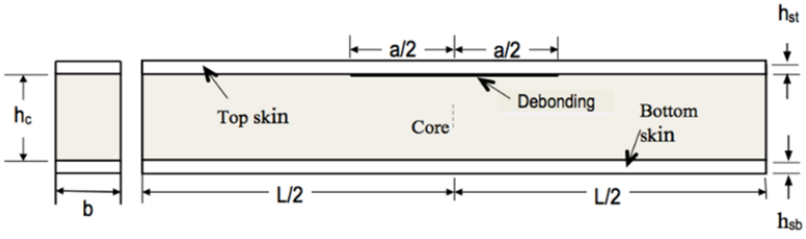

Fig. 2 Cross section and longitudinal section of the 3m sandwich beam with a central Debonding

The beam cross-section is of rectangular section with a width of b as shown in the cross section. Top and bottom skin thicknesses are h_{st} and $h_{sb,}$ respectively, and the length of the beam is L. Materials in each of the skins are assumed to be orthotropic and linear elastic. The plate element mesh for each skin lies at the horizontal plane at the mid-thickness level of the respective skin. Core material is assumed to be linear elastic, homogeneous and isotropic. Debonding is assumed to be an artificial flaw of zero thickness, embedded between top skin and core. It is assumed that debonding exists before vibration commences and stays constant without propagation during the vibration. Debonded surfaces (of skin and core) are in contact vertically but can slide in the horizontal plane to represent the contact model.

The links for the sandwich beams are of length $h_{st}/2$ where h_{st} is the thickness of the top skin. These rigid links are used for the fully bonded regions to ensure that there is no gap or sliding between the top skin and the core. In a similar manner, bottom skin is connected to the bottom surface of the core using rigid links of length $h_{sb}/2$.

III. Model Development and Validation

According to [12], contact model is of importance to prevent the interacting fragments from overlapping each other and, consequently, the modelling of the contact behaviour is necessary to properly represent the global dynamic response. Therefore master slave links in STRAND7 are used in the FE model to allow for sliding between interfaces of skin and core

in the horizontal directions while keeping skins in contact with the core in the vertical direction to effectively simulate a debonded beam according to 'contact model'. The FE model for the debonded beam is obtained by solely converting the rigid links within the debonded region to 'master slave links' in STRAND7 with assigning the proper degrees of freedom. A master-slave link defines relations between two nodes so that the displacement of the selected components will be of the same magnitude [13]. These links allow for sliding between interfaces of skin and core in the horizontal directions yet keeping skins in contact with the core in the vertical direction to mimic a debonded plate to represent the contact model.

A number of preliminary models were created and analysed before the final form described above was settled upon. The final refined model for a debonded beam is shown schematically in Fig. 3.

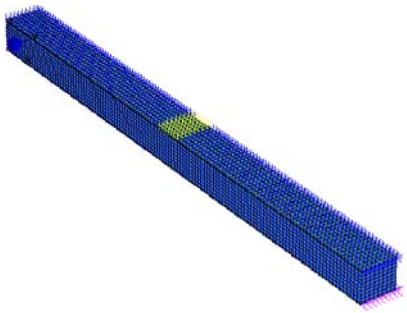

Fig. 3 STRAND7 FE model for a simply supported beam with a 30 mm full width debonding

The developed numerical model has been verified by comparing model results with published results in [14]-[16] for a foam core sandwich panel. Natural frequencies of intact (fully bonded) and debonded foam cored sandwich beams were obtained by [14] using ABAQUS FE code, and by [15], [16] using a higher order analytical approach (Modified Galerkin Method) and using ANSYS FE package. A good agreement was achieved and verification details and results obtained are reported in [11].

IV. Selection of Parameters

For the present analysis, three boundary conditions for the beam, namely, both ends simply supported (S-S), clamped-clamped (C-C) and clamped-free (C-F) have been used. Two debonding positions (debonding near the end of the beam and at centre) are considered for C-C and S-S beams whereas three positions (debonding near fixed end, at centre and near free end) are used for C-F beams. Fig. 4 explains the three debonding positions considered for C-F beams.

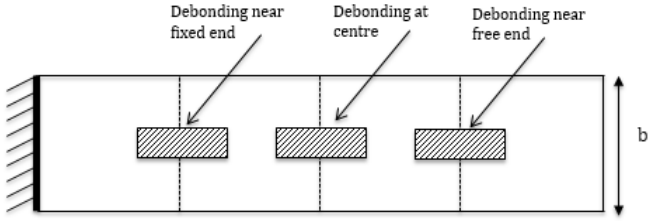

Fig. 4 Debonding positions considered for C-F beams

The relevant dimensions for the 3 m composite sandwich beam are: L = 3m, b = 200 mm, hc = 160 mm and hsb = hst = 20 mm. Debonding length 'a' varies from 30 cm to 270 cm in steps of 30 cm.

The debonding is located centrally along the length of the beam and only middle half width for scenario 1 (denoted as half width debonding), and extends through the full width of the beam for scenario 2 (referred to as full width debonding). Each beam presented here is a sandwich composite structural element mentioned in the introduction and consists of a rigid core bonded to the top and bottom glass fibre composite skins.

V. Results and Discussion

A. Influence of Extent of Debonding and End Conditions of the Beam

Table II compares the natural frequency results for the three boundary conditions (C-C, S-S and C-F) for scenario 1 (half width debonding) for the first three modes. Similarly, Table III illustrates scenario 2 results for full width debonding for the three end conditions (C-C, S-S and C-F).

TABLE II
Comparison of Natural Frequencies for the Three Boundary Conditions for Half Width Debonding

Debond	(C-C)			(S-S)			(C-F)		
length, a/L	Mode 1	Mode 2	Mode 3	Mode 1	Mode 2	Mode 3	Mode 1	Mode 2	Mode 3
0	59.228	142.121	244.031	28.978	101.526	158.087	10.669	60.916	151.753
0.1	59.227	141.873	243.996	28.978	101.384	158.04	10.668	60.915	151.429
0.2	59.219	141.588	243.647	28.977	101.207	157.971	10.665	60.907	151.053
0.3	59.195	141.432	242.836	28.975	101.081	157.896	10.663	60.885	150.841
0.4	59.147	141.394	241.892	28.97	101.016	157.814	10.661	60.842	150.78
0.5	59.072	141.385	241.284	28.962	100.997	157.727	10.659	60.778	150.772
0.6	58.971	141.284	241.136	28.951	100.994	157.638	10.657	60.696	150.69
0.7	58.846	140.99	241.075	28.937	100.97	157.551	10.655	60.6	150.448
0.8	58.707	140.468	240.53	28.92	100.895	157.464	10.653	60.499	150.043
0.9	58.557	139.765	239.218	28.898	100.732	157.377	10.651	60.398	149.548

It is observed from the comparison of fully bonded frequencies (when debonding length a/L is zero) of Tables II and III that C-C end condition has the highest frequency values indicating the highest stiffness whereas C-F beam

shows the least stiffness. It is also revealed that full width debonding causes drastic changes to natural frequencies compared to fully bonded beams due to immense loss of stiffness due to full width debonding.

Comparison of full width and half width debonding as indicated by frequency values in Tables I-III reveals that half width debonding has much lesser effects on natural frequency compared to full width debonding.

A closer look at the vibration modes and their corresponding mode shapes divulges that debonding cause changes in modes of vibration in some modes and these changes are more pronounced in full width debonding than half width debonding. More participation of twisting modes are perceived in full width debonding as demonstrated in Figs. 5-7 where notable changes observed in C-C, S-S and C-F end conditions respectively are exemplified. Fig. 5 illustrates the mode shape comparison for 4th mode of vibration for the C-C beam. It is stimulating to see that the sway mode for fully bonded beam is changed to a bending mode in half width debonding while full width debonding causes it to change to a mixed bending and twisting mode.

TABLE III
COMPARISON OF NATURAL FREQUENCIES FOR THE THREE BOUNDARY CONDITIONS FOR FULL WIDTH DEBONDING

Debond	(C-C)			(S-S)			(C-F)		
length a/L	Mode 1	Mode 2	Mode 3	Mode 1	Mode 2	Mode 3	Mode 1	Mode 2	Mode 3
0	59.228	142.121	244.031	28.978	101.526	158.087	10.669	60.916	151.753
0.1	59.225	140.174	243.894	28.978	100.414	157.727	10.657	60.909	149.206
0.2	59.171	132.098	241.364	28.972	95.404	156.191	10.595	60.836	138.667
0.3	58.871	120.355	230.144	28.943	86.498	153.775	10.448	60.498	123.481
0.4	57.916	111.095	209.759	28.848	76.89	150.578	10.195	59.515	111.089
0.5	55.767	106.527	191.646	28.615	68.994	144.213	9.831	57.455	103.825
0.6	52.133	105.528	182.633	28.156	63.354	134.737	9.373	54.174	100.744
0.7	47.315	105.172	181.052	27.387	59.735	127.042	8.851	50.008	99.921
0.8	42.01	101.848	179.504	26.272	57.746	123.009	8.297	45.531	99.119
0.9	36.858	94.271	170.68	24.791	56.999	121.84	7.742	41.231	96.571

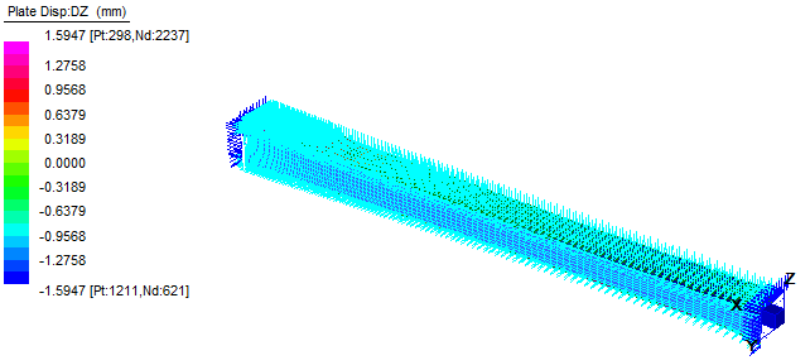

(a) C-C fully bonded beam (sway mode)

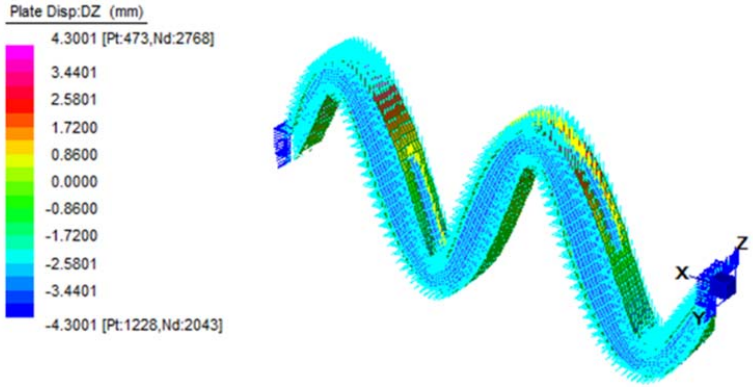

(b) C-C 150 cm long half width debonding (bending mode)

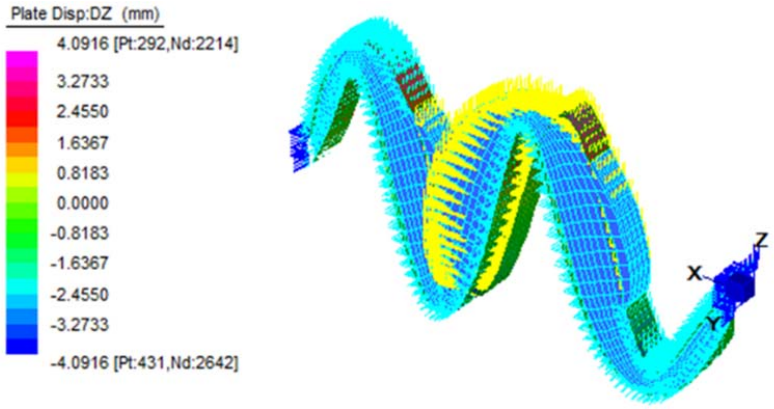

(c) C-C 150 cm long full width debonding (mixed mode; bending and twisting)

Fig. 5 Comparison of mode shapes for mode 4 in C-C beam

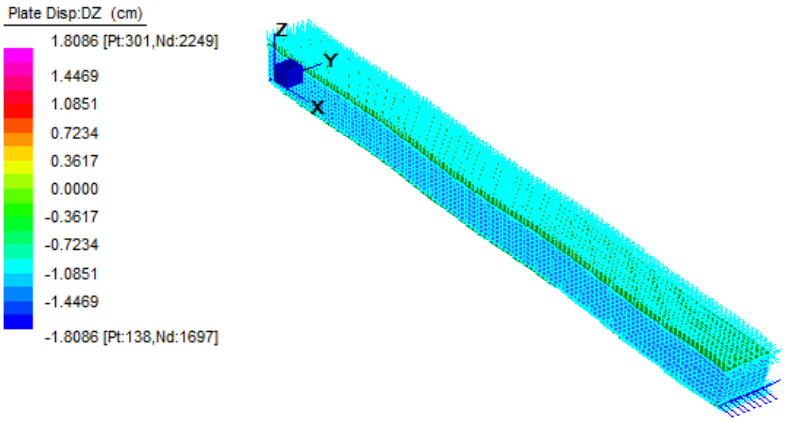

(a) S-S fully bonded beam (longitudinal mode)

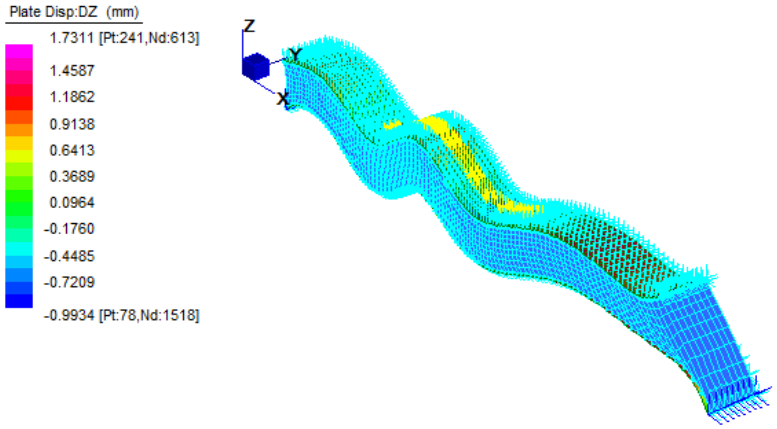

(b) S-S half width 150 cm long debonding (bending mode)

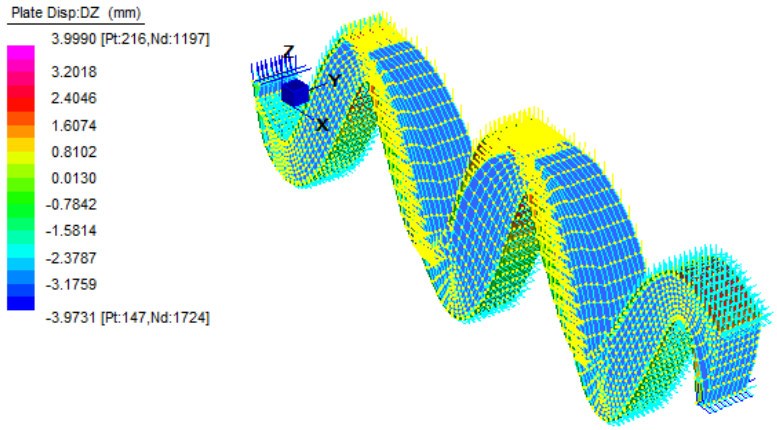

(c) S-S full width 150 cm long debonding (bending mode)

Fig. 6 Comparison of mode shapes for mode 7 in S-S beam

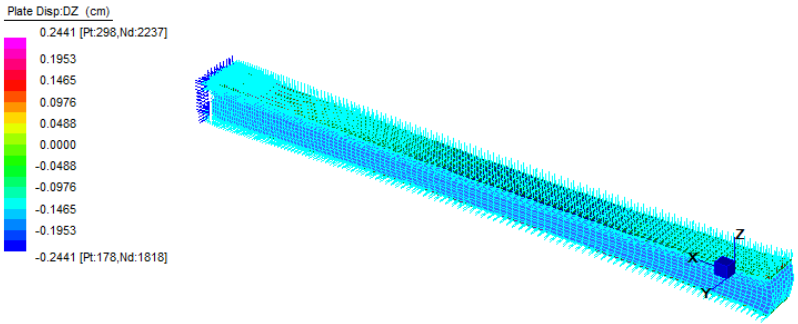

(a) C-F fully bonded beam (longitudinal mode)

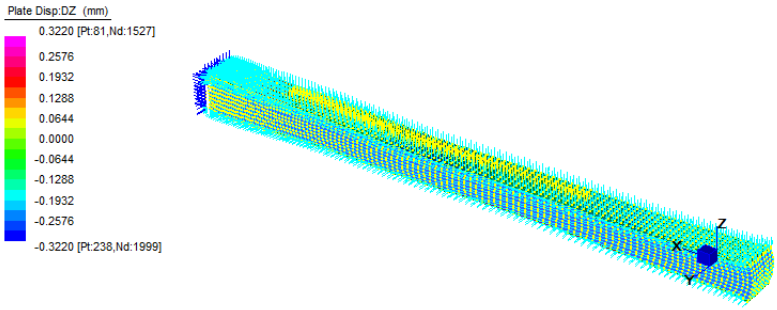

(b) C-F half width 150 cm long debonding (sway mode)

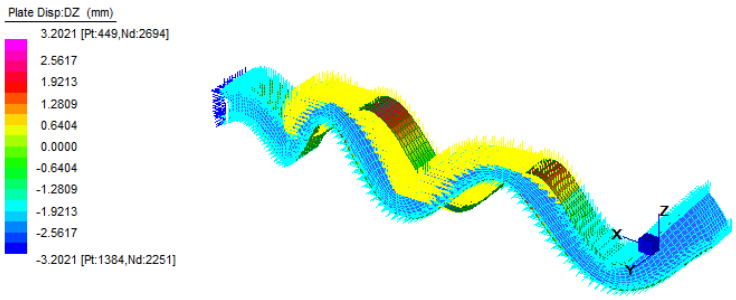

(c) C-F Full width 150 cm long debonding (mixed mode; bending and twisting)

Fig. 7 Comparison of mode shapes for mode 8 in C-F beam

Fig. 6 shows the mode shapes for mode 7 in S-S beam where fully bonded beam is compared with half width and full

width debonding cases. There the longitudinal mode for fully bonded beam changes to a bending mode in half width and full width debonding. Fairly similar scenario to C-C beam occurs in C-F beam mode 8 comparison as revealed from Fig. 7. In that situation, half width debonding does not cause any change in vibration mode, yet full width debonding sources dramatic modifications giving very high lateral displacements compared to fully bonded and half width debonded cases, producing combined bending and twisting vibration mode.

B. Influence of Extent of Debonding and End Conditions of the Beam

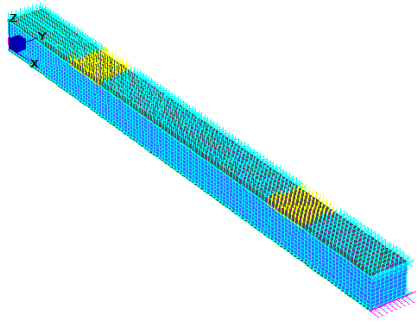

(a) S-S beam with two equally sized (each 30 cm long full width) debonding regions

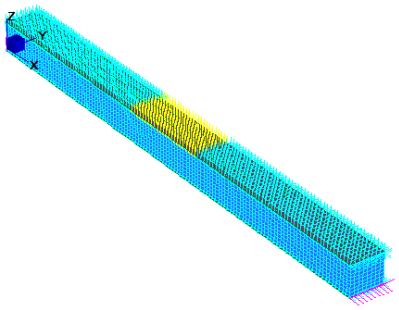

(b) S-S beam with equivalent single debonding region (60 cm long full width debonding)

Fig. 8 FE models generated with STRAND7 for S-S beam (for Fig. 11 comparison)

In this section, influence of double (two equally sized debonding zones positioned near two ends as illustrated in Fig. 8) debonding on natural frequency reduction is examined for full width and half width debonding scenarios. Secondly, comparisons are made between multiple debonding and equally sized single debonding.

Fig. 9 illustrates the comparison of natural frequency variation for full width and half width debonding for 30 cm double debonding (two 30 cm long debonding zones near the two ends) in the C-C beam, whereas Fig. 10 shows the same variation for S-S beam.

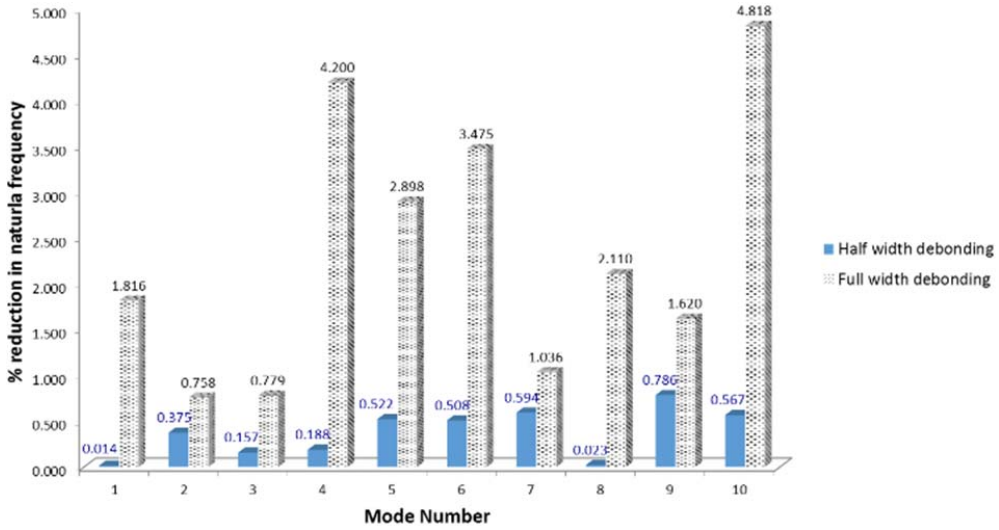

Fig. 9 Comparison of full width and half width debonding for C-C beam with 30 cm double debonding

It is evident from both Fig. 9 and Fig. 10 that full width debonding causes enormous changes in natural frequency compared to half width debonding for similar scenarios. These variations do not follow a monotonically increasing pattern with the mode number, as demonstrated by Figs. 9 and 10.

Comparison of Figs. 9 and 10 also reveals that for the first four modes, the variations for full width compared to half width debonding is more significant for C-C case, and on contrary, higher modes shows more variations for S-S case than C-C case.

Fig. 11 compares effects of two equally sized (30 cm long full width debonding regions each) symmetrically located debonding zones and equivalent single debonding (full width) for S-S beam. It is evident from Fig. 11 that single debonding of 60 cm length generally gives higher extent of reduction in natural frequency than two equally sized 30 cm long debonding regions. These percentage reductions do not seem to increase monotonically with the increase of the mode number. This is evident from the similar comparison for C-C beam as well, as illustrated in Fig. 12.

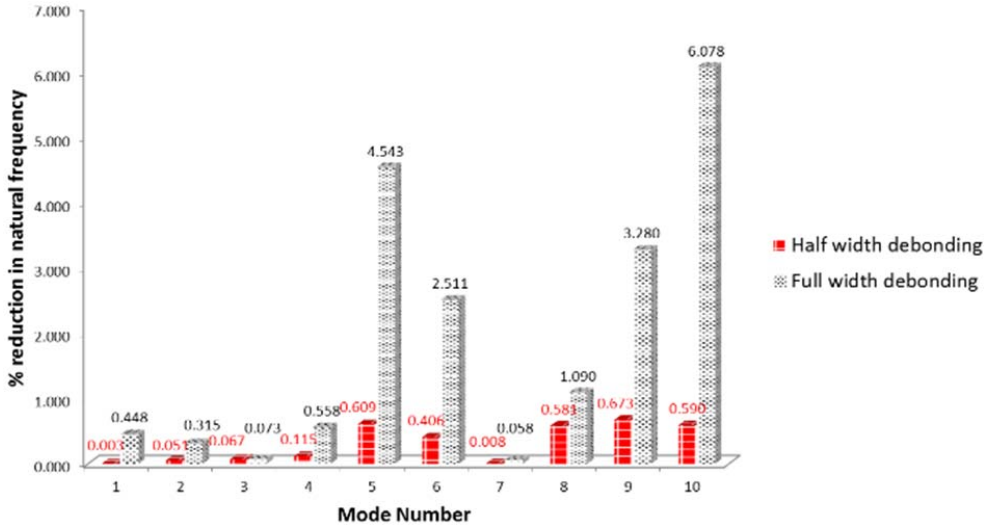

Fig. 10 Comparison of full width and half width debonding for S-S beam with 30 cm double debonding

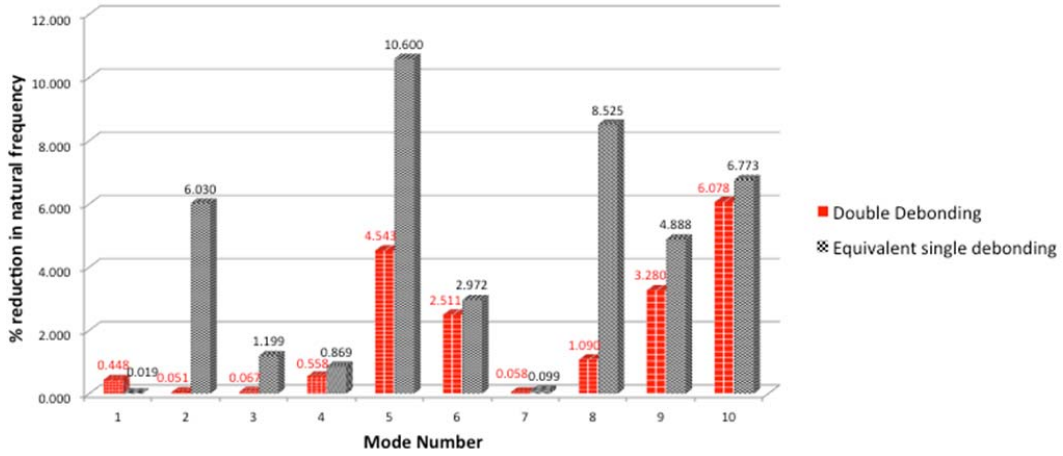

Fig. 11 Comparison for double debonding and equivalent single debonding for S-S beam

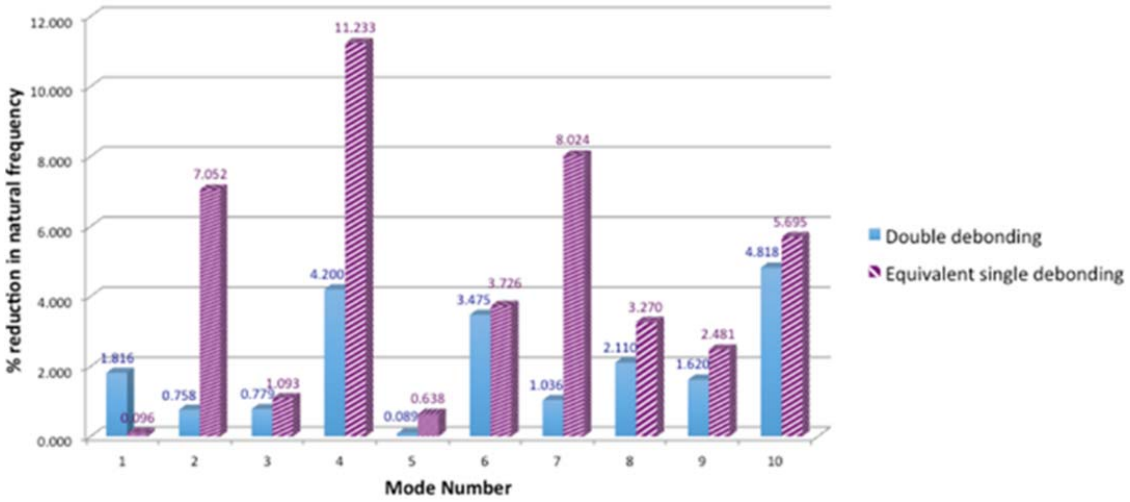

Fig. 12 Comparison for double debonding and equivalent single debonding for C-C beam

C. Influence of Triple Debonding

The comparison of triple debonding, 30 cm long each, symmetrically located along the length (as illustrated in Fig. 13) with equivalent single debonding of 90 cm for C-C beam is displayed in Fig. 14. Figs. 13 (a) and 13 (b) show the FE

models generated with STRAND7 for the two scenarios.

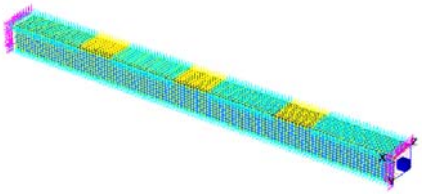

(a) Triple debonding 30 cm each

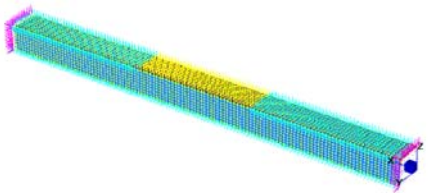

(b) Equivalent single debonding 90 cm long

Fig. 13 FE models generated with STRAND7 for C-C beam for triple debonding and equivalent single debonding

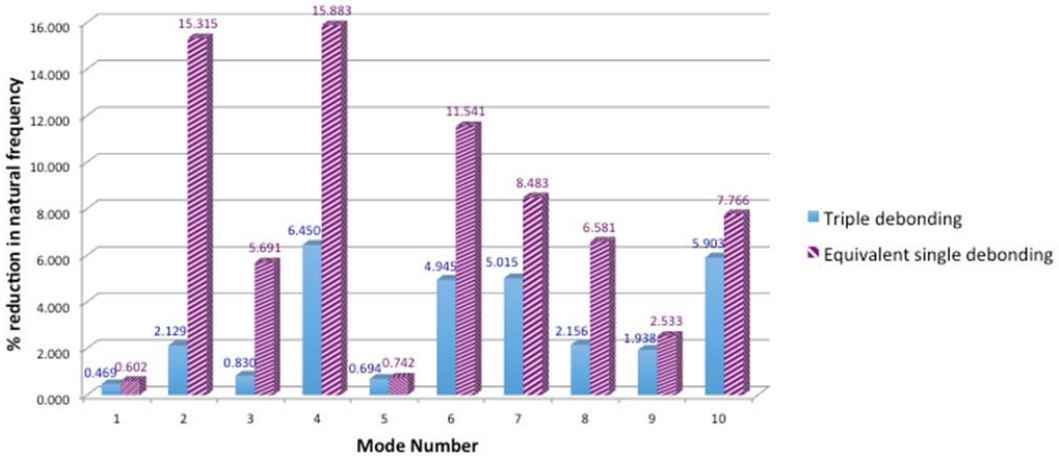

Fig. 14 Comparison of triple debonding and equivalent single debonding for C-C beam

Fig. 14 compares triple debonding with an equivalent area of single debonding for a beam with C-C boundary conditions. It is evident from Fig. 14 that, equivalent single debonding affects the free vibration frequencies way more than that of the isolated triple debonding of the same area, generally in the order of more than two times in most of the modes under consideration.

VI. Conclusions

i. Although there is a general tendency that the extent of natural frequency reduction with respect to debonding increases with the mode number, this does not always exhibit an increasing trend as the mode number increases, but follows different trends depending on the boundary condition, extent of debonding and location of the debond.
ii. The decrease in natural frequency with the increase in the extent of debonding is more dependent on the width of debonding across the beam than the length along the beam for the composite beam considered in the analysis.
iii. A debonding located near the end of the beam significantly worsens the free vibration characteristics compared to a debonding located near the centre of the beam. This becomes more pronounced when the beam is more restrained.
iv. For similar extents and locations of debonding, the effect of debonding on natural frequencies seems significantly dependent on the end conditions of the beam, giving higher reduction in natural frequency when the beam is more restrained. Hence it is revealed that the stronger the supports are restrained, the bigger the influence on dynamic characteristics.
v. It is observed that full width debonding attributes to extremely severe reduction in natural frequency compared to half width debonding for all three support conditions considered. Full width debonding also attributes to drastic changes in modes of vibration and mode shapes.
vi. The effect of double debonding on the free vibration behaviour of a debonded beam is highly dependent of the boundary conditions, giving greater reductions in natural frequencies when the beam is more restrained.
vii. It is also observed that the reduction in natural frequency is more affected by single debonding than the equally sized double debonding located symmetrical to the single debonding position.

References

[1] D. Elmalich, and O. Rabinovitch, "A high-order finite element for dynamic analysis of soft-core sandwich plates," Journal of Sandwich Structures & Materials, vol. 14, no 5, pp.525–555, 2012.
[2] Jansons, V.Kulakov, A. Aniskevich, and Lagzdiņš. "Structural composites − from aerospace to civil engineering applications," Innovations and Technologies News, vol. 17, pp3-12, 2012.
[3] A.K Gand, T. M. Chan, T. Mottram, (2013). "Civil and structural engineering applications, recent trends, research and developments on pultruded fiber reinforced polymer closed sections: a review" Front. Struct. Civ. Eng., 7(3): 227–244.
[4] V. Rizov, A. Shipsha, D. Zenkert, "Indentation study of foam core composite composite panels," Compos. Struct, vol 69, pp 95-102, 2005.

[5] V. N. Burlayenko and T. Sadowski, "Linear and Nonlinear Dynamic Analyses of Sandwich Panels with Face Sheet-to-Core Debonding," Shock and Vibration, vol. 2018, Article ID 5715863, 26 pages, 2018. https://doi.org/10.1155/2018/5715863

[6] A.C.Manalo, T. Aravinthan, W. Karunasena, "Flexural behaviour of glue-laminated fibre composite sandwich beams," Composite Structures, vol 92, pp 2703–2711, 2010.

[7] A.C.Manalo, T. Aravinthan, W. Karunasena, M.M.Islam, "Flexural behaviour of structural fibre composite sandwich beams in flatwise and edgewise positions," Composite Structures, vol 92 (4), pp 984-995, 2010.

[8] M.M. Islam, T. Aravinthan, "Behaviour of structural fibre composite sandwich panels under point load and uniformly distributed load,"Composite Structures, 93, pp 206–15, 2010.

[9] Z.K. Awad, T. Aravinthan, Y. Zhuge, "Experimental and numerical analysis of an innovative GFRP sandwich floor panel under point load," Engineering Structures, vol 41, pp 126–135,2010.

[10] W. Karunasena, The effect of debonding on the natural frequencies of laminated fibre composite sandwich plates. Proceedings of 6th Australasian Congress on Applied Mechanics, ACAM 6 , 12-15 December 2010, Perth, Australia, 2010.

[11] I. Jayatilake , W. Karunasena and W. Lokuge, "Dynamic behaviour of debonded GFRP composite beams," Journal of Multifunctional Composites, vol. 1 (2), pp. 113-122, 2013.

[12] V. N. Burlayenko and T. Sadowski, "Finite element nonlinear dynamic analysis of sandwich plates with partially detached facesheet and core," Finite Elements in Analysis and Design, vol 62, pp 49-64, 2012.

[13] STRAND7, Strand7 finite element analysis FEA software, Release 2.4.1, Sydney, Australia J. 2010, (website: www.strand7.com).

[14] V. N. Burlayenko and T. Sadowski, "Dynamic behaviour of sandwich plates containing single/multiple debonding," Computational Materials Science, vol 50 (4), pp 1263-1268, 2011.

[15] G.H. Schwarts, O. Rabinovich, Y. Frostig, "Free vibrations of delaminated unidirectional sandwich panels with a transversely flexible core-a modified Galerkin approach,". Journal of Sound and Vibration, vol 301, pp 253-277,2007

[16] G.H. Schwarts, O. Rabinovich, Y. Frostig, "Free vibration of delaminated unidirectional sandwich panels with a transversely flexible core and general boundary conditions - A high-order approach," Journal of Sandwich Structures & Materials, vol 10, pp 99-131, 2008.